

Simultaneous Localization and Mapping Using Ambient Magnetic Field

Ilari Vallivaara, Janne Haverinen, Anssi Kemppainen, Juha Röning
Computer Science and Engineering Laboratory, University of Oulu, Finland

firstname.lastname@ee.oulu.fi

Abstract—In this paper we propose a simultaneous localization and mapping (SLAM) method that utilizes local anomalies of the ambient magnetic field present in many indoor environments. We use a Rao-Blackwellized particle filter to estimate the pose distribution of the robot and Gaussian Process regression to model the magnetic field map. The feasibility of the proposed approach is validated by real world experiments, which demonstrate that the approach produces geometrically consistent maps using only odometric data and measurements obtained from the ambient magnetic field. The proposed approach provides a simple, low-cost, and space-efficient solution for solving the SLAM problem present in many domestic and swarm robotics application domains.

I. INTRODUCTION

Simultaneous Localization and Mapping (SLAM) is one of the most fundamental challenges in mobile robotics. In SLAM the robot has no prior map nor pose information, and it tries to simultaneously acquire a map and localize itself. In addition to odometric information, sensor information from the surrounding environment is also needed in SLAM in order to compensate the effect of cumulative error introduced by odometric sensors. Recently, much work has been done with sonar and laser based SLAM approaches, which already provide viable solutions for the SLAM problem, e.g. [1], [2], [3], [4]. However, to the best of our knowledge, this is the first time the spatial anomalies of indoor magnetic fields have been utilized to solve the SLAM problem, yielding a low-cost, simple, and space-efficient SLAM solution for cost- and space-sensitive application domains.

Particularly, low-cost domestic robots such as robotic vacuum cleaners would benefit from inexpensive and computationally efficient SLAM methods. While some domestic robots use sophisticated navigation, most of them still rely very much on randomized actions, which in cleaning tasks can result in overcleaning [5], for example. Some work has been done on implementing SLAM or plain global localization with agents that have very limited sensing capabilities. In [6] the SLAM problem is tackled with very sparse laser readings, while [7] reports SLAM capabilities of an unmodified Roomba. Our method does not go as far as the blind robot localization in [8], but is more close e.g. to the underwater robot navigation approach proposed in [9], both having similar sensor setting, providing information only from one point in space at a time.

Deviations in indoor magnetic fields caused by electrical devices or ferromagnetic structures in buildings [10] have usually been considered as a source of error for magnetic

sensors, such as compasses [11], [12]. However, some authors have suggested that these anomalies could be utilized as useful features instead. In [13], the deviations of compass headings were used to provide distinctive location signatures. In [14], the authors consider the local properties of a magnetic field as a spatially changing physical quantity and use a particle filter to perform one-dimensional global localization of the robot by utilizing a magnetic map of the environment, which has been generated manually prior to the localization. Although the experiments presented here somewhat further the results presented in [14] into two-dimensional case, global localization is beyond the scope of this paper and will be addressed elsewhere.

Due to the fact that any SLAM solution is based on information available from the environment, through the use of sensors, which provides consistent evidence about spatial locations it is a plausible assumption that the ambient magnetic field can be used as a source of information in order to solve the SLAM problem. In this paper, we present a proof of concept of a SLAM approach that is based solely on the utilization of measurements made from the ambient magnetic field in addition to odometric information. The experiments reported in this paper demonstrate that by using an unsophisticated low-cost sensor setup it is possible to obtain geometrically consistent maps for indoor environments. A theoretical analysis of the results will be addressed elsewhere.

II. AMBIENT MAGNETIC FIELD BASED SLAM

A. Outline

The main hypothesis of the proposed approach is that an indoor ambient magnetic field contains enough information to overcome the cumulative error of odometry data. Our experiments suggest that this hypothesis is valid, and that the magnetic landscape has enough deviation to correct the odometry information (see Fig. 1). In our experiments, the robot randomly wanders in an environment while performing SLAM. A Rao-Blackwellized particle filter [15], [1], [16] is used to estimate the map and the pose of the robot. We make the assumption that the three orthogonal components of the magnetic vector field can be independently modeled by using Gaussian process (GP) regression [17]. When a particle returns to a previously visited area, a local model of the magnetic field is generated by using the previous measurements available from the surrounding locations (see Fig. 2). The local model is used to obtain a measurement

prediction at the pose represented by the particle. This prediction is then compared to the actual measurement made by the magnetometer of the robot in the true pose to determine the measurement probability and the corresponding weight of the particle. The method relies strongly on loop closings due to characteristics of magnetic field measurements and it could considerably profit from active loop closing strategies [18], [16]. In this paper we simply rely on random motion of the robot in order to ensure an adequate amount of loop closings.

In each time step the following actions are performed

- 1) Model the odometry for each particle
- 2) Generate local model of each particle's map according to earlier measurements
- 3) Use the local model to compute predicted reading for each particle
- 4) Use the predicted reading to compute the likelihood of the most recent measurement for each particle
- 5) Update particle weights according to the likelihood, and normalize weights
- 6) Resample the particle cloud according to the particle weights (if necessary)
- 7) Update the GP parameters for every particle (namely the initial mean is set to mean of measurements)
- 8) Update particle maps

B. Gaussian Processes

The magnetic vector field is modeled by three independent Gaussian processes (see [17]), which generalize multivariate normal distributions into metric sensing spaces. The three vector components (f_x, f_y, f_z) are now given by

$$f_i(x) \sim \mathcal{GP}(m_i(x), k_i(x, \hat{x})) \quad (1)$$

where i denotes vector component, $m_i(x)$ is a mean function and $k(x, \hat{x})$ a covariance function. For each vector component, we used a constant mean function and a squared exponential covariance function given by

$$k_i(x, \hat{x}) = \sigma_i^2 \cdot \exp\left(-\frac{|x - \hat{x}|^2}{l^2}\right) \quad (2)$$

where σ_i^2 is a signal variance hyperparameter and l^2 a length-scale hyperparameter. The complexity of Gaussian process regression is $O(n^3)$, where n is the number of datapoints. The computational complexity of the GP regression in the proposed method is controlled by defining a threshold for the number of surrounding data points used in the regression. The hyperparameters for GPs were approximated by using the magnetic field data previously collected from the Computer Science and Engineering Laboratory. Lengthscale l for GPs was set to $l = 1.0$ (m), and signal variances for x , y , and z vector components were set to $\sigma_x^2 = 1.4$, $\sigma_y^2 = 1.4$, and $\sigma_z^2 = 0.69$, respectively.

C. Particle filter

We used a Rao-Blackwellized particle filter [15], [1], [16] to estimate the trajectory of the robot and the magnetic field map. A Rao-Blackwellized particle filter estimates the

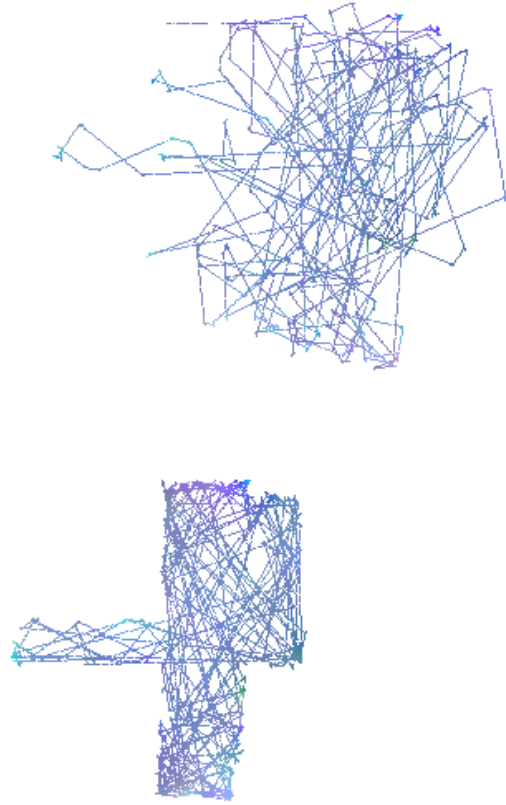


Fig. 1. Trajectory based on raw odometry (above). Corrected trajectory (below).

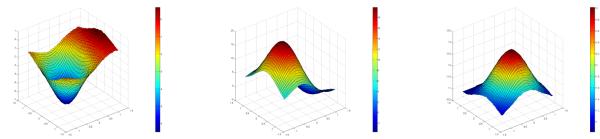


Fig. 2. An example of a local model of the magnetic field predictions modeled by three independent Gaussian processes (x , y , and z from left to right).

posterior $p(x_{1:t}|z_{1:t}, u_{0:t})$ about potential trajectories $x_{1:t}$ of the robot when having measurements $z_{1:t}$ and odometric information (control) $u_{0:t}$. This posterior is then used to compute the posterior

$$p(x_{1:t}, m|z_{1:t}, u_{0:t}) = p(m|x_{1:t}, z_{1:t})p(x_{1:t}|z_{1:t}, u_{0:t}). \quad (3)$$

over maps and trajectories. The posterior $p(x_{1:t}|z_{1:t}, u_{0:t})$ shown in Eq. 3 is approximated with particles $\{x_t^{(i)}\}$, in which each particle x_t^k is associated with a map $m^{[k]}$, built according to measurements $z_{1:t}$ and trajectory $x_{1:t}$ of the corresponding particle. The proposal distribution for trajectories is drawn from the probabilistic motion model.

We use a simplified version of the odometry motion model described in [16] by modeling the odometry by a

translation followed by a single rotation. This version of the motion model is in practice identical to the model described in [16], because in our experiments we do not rotate the robot while driving forward and we apply the motion model frequently. For the same reasons, we use relatively large standard deviation for the straight motion and the rotation noise ($\alpha_1 = \alpha_3 = 0.15$) and a small value or zero for cross terms ($\alpha_4 = 0$ and $\alpha_2 = 0.0001/r$, where r is the radius of the robot). The chosen values agree with those reported in [7]. In our experiments, we do not take into account the possible odometric error caused by collision with walls, as is suggested e.g. in [7]. However, this seems to be no issue for the proposed method.

For resampling we use Residual Resampling [19] that is called every time the effective sample size [20] $N_{eff} = 1/\sum_{i=1}^M (w^i)^2$ drops below $0.5M$, as suggested in [2], where M is the number of particles.

D. Map representation and local model

1) *Map*: The map m is defined as a two-dimensional grid, with each cell containing information of the measurements made in it. In our experiments the grid resolution is chosen to be $5cm \times 5cm$. Each observation \mathbf{z} associated with a cell contains the location of the observation point z_c , timestamp z_{ts} , and the value of the magnetic field $\mathbf{z}_{x,y,z} = [z^x, z^y, z^z]$ at the observation point, consisting of the three components of the magnetic flux density (in μT) in x , y , and z directions, respectively. Each observation made from the magnetic field is transformed into the arbitrary world coordinate system represented by the particular map.

In our experiments, we found that raising the number of measurements associated with a single cell beyond a certain point did not improve the localization performance. It seems that new measurements do not provide significant contribution to the data from an information point of view. Therefore we limit the number of measurements associated with a single cell as a tradeoff between map accuracy and map memory usage. We noticed that by allowing less than 3 measurements inside a cell the localization performance suffers considerably, especially near walls where there can be many measurements inside a single cell. This is due to the fact that robot rotates in place near walls prior advancing towards free space. In our experiments, the limit was set to 5 measurements, older measurements being replaced at random when newer ones are added.

2) *Local model*: The local model represents the magnetic landscape in the local neighborhood of a particle. The local model is defined as a vector of three Gaussian processes, $\mathcal{GP}_{x,y,z} = [\mathcal{GP}^x, \mathcal{GP}^y, \mathcal{GP}^z]$. The prior mean for these GPs is obtained using the mean of corresponding measurements $z_{1:t}^i$. The Gaussian processes are used to model the three orthogonal components of the magnetic flux density in x , y , and z directions, respectively. The local model is used to make predictions of the magnetic field and to compute the likelihood $p(z_t|x_t^k, m^{[k]})$ of the observation z_t conditioned on the pose x_t^k and the map $m^{[k]}$. This is then used to compute the posterior over maps $p(m|x_{1:t}, z_{1:t})$ in (3). Let

$\mathbf{m}(x_t^k) = [m_x(x_t^k), m_y(x_t^k), m_z(x_t^k)]$ be a vector of values of the mean predictions from the corresponding Gaussian processes. Due to the independence assumption, the measurement probability $p(z_t|x_t^k, m^{[k]})$ is estimated as a product of the likelihood of the magnetic x , y , and z components z_t^x , z_t^y , and z_t^z of observation z_t . These likelihoods are determined, after rotating the measurement to the coordinate system of the map, by a normal distribution with mean of $m_i(x_t^k)$ and standard deviation σ_i , i.e.

$$p(z_t|x_t^k, m^{[k]}) = \prod_{i=x,y,z} \frac{1}{\sigma_i} \phi\left(\frac{z_t^i - m_i(x_t^k)}{\sigma_i}\right) \quad (4)$$

We experimentally studied the effect of using different values for the standard deviation σ_i . If the predicted variance provided by the GP was used to estimate σ_i , the variance of particle weights increased significantly which had an adverse effect to the diversity of the particle distribution in unexplored areas. Instead, we used an experimentally specified constant value of $\sigma = 3.0$, found by trial and error, for the standard deviation for all particles. The constant value was found to capture the uncertainty of the local model well. We noticed that there is a lot of room for further research in the selection of σ_i , as it fundamentally affects the particle weights and for example controls the aggressiveness of resampling.

3) *Local model datapoint selection*: The local model for each particle x_t^k is generated using a fixed number of measurements in the local neighborhood of the particle (see Fig 3). These measurements are given to the corresponding GP in $\mathcal{GP}_{x,y,z}$ as datapoints. In order to get approximately evenly distributed datapoints from the local neighborhood of the particle, the neighborhood is divided into four sectors (up, down, right, left), each sector having field of view of 90 degrees. The fixed number of datapoints, distributed among the sectors as evenly as possible, is then chosen from these sectors. Datapoints inside each sector are chosen by distance in ascending order. In our experiments we used a total maximum of ten datapoints for each model (including all sectors) accepting only the datapoints whose distance were less than the predefined distance threshold which was set to $0.5m$. The sample selection method described above is not computationally involved and was therefore used to approximate more complex approaches. We will address later the issue of developing more sophisticated methods for sample selection.

In our experiments we noticed that the closest (usually most recent) measurements dominate the local model, and that the most recent measurements give overly optimistic likelihood values especially in unexplored areas. To alleviate this problem we introduce a criterion called *tabu time* t_{tabu} . This criterion is used to discard such measurements z from the measurement selection process that solve the inequality $z_{ts} + t_{tabu} > t$, where t is the current time. The use of t_{tabu} places more importance on older measurements and makes the loop closing a more consistent which clearly improves the performance of the method. When choosing the value for t_{tabu} , one should consider both the robot's speed and

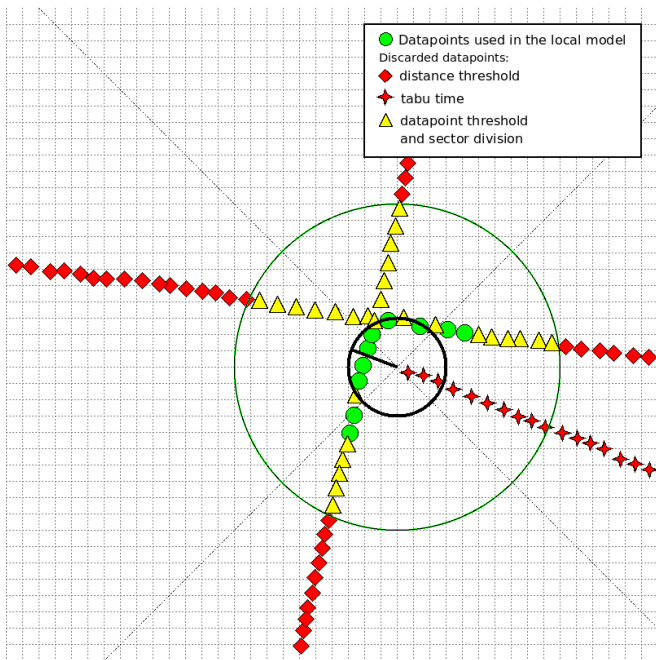


Fig. 3. Local model datapoint selection. Ten datapoints are selected according to the criteria described in II-D.3.

selection distance threshold. In our experiments, $t_{tabu} = 10s$ was used which was experimentally found to prevent the overly optimistic likelihoods in unexplored areas and to allow a turning robot to utilize nearby measurements in order to estimate its heading at the same time.

Another notable thing in sparsely mapped magnetic environments is that when there are not enough datapoints available for the Gaussian process, using the local model for weight computation will bias the heading in some direction. Therefore, when there is no datapoints to be used within the measurement selection threshold we update the particle's weight by using the mean likelihood of the particles that have measurements in their neighborhood. If none of the particles can use the local model, the weights are not updated.

III. EXPERIMENTS

A. Data collection and experimental setup

The real world data collection was conducted using an iRobot Create mobile robot platform equipped with a MicroMag 3-axis magnetometer shown in Fig. 4 and described in [14]. The magnetometer was calibrated using the method described in [14] to obtain non-biased measurements. For the automated data collection we wrote a simple algorithm to randomize the motion of the robot. The algorithm controls the robot to drive in a straight line at a velocity of $10cm/s$ until its tactile sensors are activated due to collision with an obstacle. After the collision, the robot moves $5cm$ backwards and rotates at a random angle in the direction opposite to the active tactile sensor (left or right). The data was collected until the robot ran out of battery power (this took approximately 2.5 h). The collected data was then downsampled using a median filter to reduce the observation

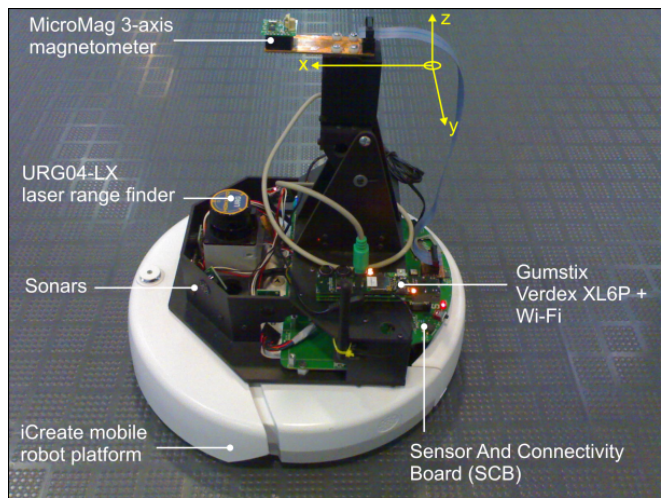


Fig. 4. iRobot Create used in the experiments. Only magnetometer data and odometry information were used in the experiments.



Fig. 5. The CSE lobby

frequency to $2Hz$. The experiments were repeated in two different environments.

B. Results

The first environment where the SLAM experiments were conducted was the lobby of the Computer Science and Engineering (CSE) Laboratory shown in Fig. 5. The CSE laboratory is located in a modern office building whose frame structure has been build of steel and reinforced concrete structures, which has a significant impact on the ambient magnetic field observed inside the building. By using 200 particles the proposed approach was able to produce geometrically consistent maps in 19 cases out of 20 as is illustrated in Fig. 6. The consistency of the generated maps was verified visually by superimposing the map to the floor plan of the experiment environment. The success rates with different particle counts are presented in Table I. The proposed method is able to consistently produce similar magnetic field maps in separate experiments as is illustrated in Fig. 7.

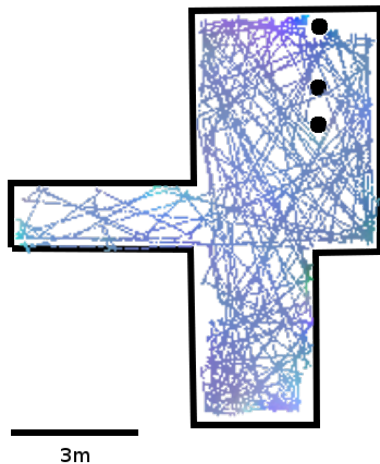


Fig. 6. The floor plan of the CSE laboratory has been superimposed to the trajectory data produced by a successful experiment. The unexplored areas near walls (upper-right and lower-right corners) correspond to book shelves in the lobby. Also the unexplored area near the plant (visible in Fig. 5) can be recognized from the map (low-left).

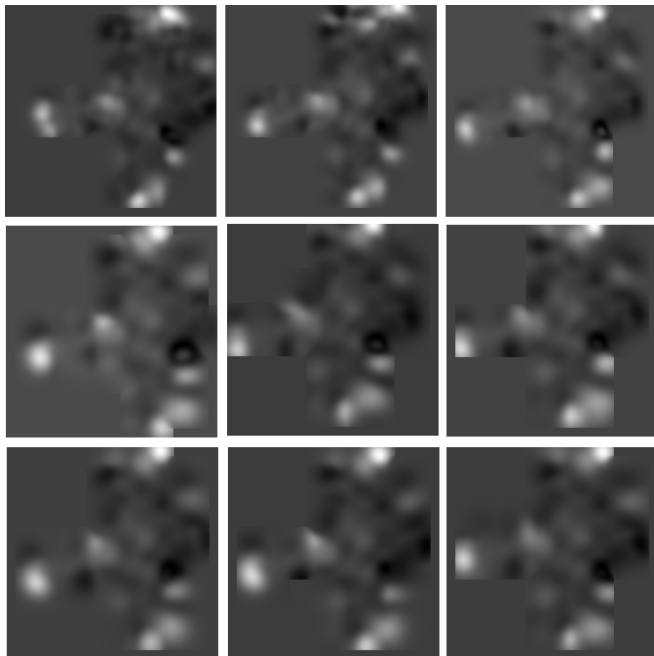


Fig. 7. Comparison of obtained magnetic maps (norm) in separate successful experiments conducted in the CSE laboratory.

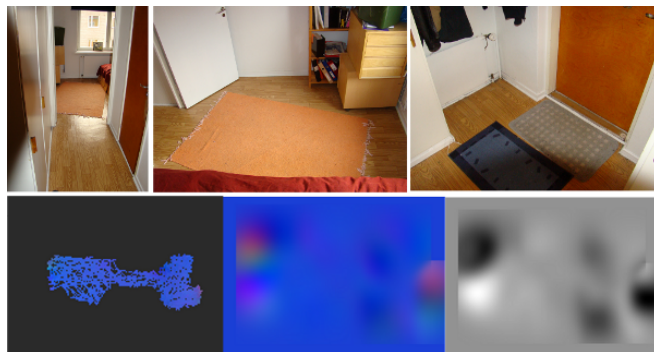


Fig. 8. The second experiment environment. The two radiators of the apartment shown in pictures (up-right, up-left) can be clearly seen in the obtained maps (bottom-middle, bottom-right). The map in the center is plotted using x , y and z as rgb -values, respectively, while the map on the right represents the norm of the magnetic field.

TABLE I
SUCCESS RATES OF OUR METHOD WITH DIFFERENT AMOUNT OF PARTICLES, DATASET CSE LOBBY

Number of particles	Success rate
200	19/20
150	16/20
100	14/20
50	6/20

The second experiment environment was a two-room apartment, shown in Fig. 8, in the third floor of an apartment house which has been build in the 1950s. The ferromagnetic structures in this environment were not so obvious. However, because of the smaller size of this environment (furthest distance from corner to corner about $5,5 m$) the two radiators in separate rooms were probably enough to reset the odometry frequently enough to have similar success rates as in the experiments conducted in the CSE laboratory. The edges in the maps were not as clear as in the maps generated in CSE laboratory, but the geometric structure was clearly captured and tracking worked well after the map was created.

IV. CONCLUSIONS

In this paper we have presented a proof of concept which demonstrates that indoor SLAM method can be implemented by utilizing observations made from the ambient magnetic field using a low-cost magnetometer. We argue that many modern buildings have the required ambient magnetic field characteristics in order to successfully apply the proposed method in different spatial scales.

In this paper the mapped areas were relatively small compared to laser-based SLAM methods, but using active loop closing (e.g. [18]), methods for low structured environments (e.g. [4]), active localization, and robust SLAM exploration strategies, it should be possible to scale up the area to be explored considerably. This is an issue which we will address in our future work.

The proposed approach can be useful in swarm robotics, miniature multi-robot systems, and in multi-robot SLAM due

to its cost-efficient and space-efficient characteristics.

REFERENCES

- [1] Michael Montemerlo and Sebastian Thrun. *FastSLAM: A Scalable Method for the Simultaneous Localization and Mapping Problem in Robotics (Springer Tracts in Advanced Robotics)*. Springer-Verlag New York, Inc., Secaucus, NJ, USA, 2007.
- [2] G. Grisetti, C. Stachniss, and W. Burgard. Improving grid-based slam with rao-blackwellized particle filters by adaptive proposals and selective resampling. pages 2443–2448, 2005.
- [3] Dirk Hähnel, Wolfram Burgard, Dieter Fox, and Sebastian Thrun. An efficient fastslam algorithm for generating maps of large-scale cyclic environments from raw laser range measurements. In *In proc. of The IEEE/RSJ Int. Conf. On Intelligent Robots And Systems (IROS)*, pages 206–211, 2003.
- [4] Slawomir Grzonka, Christian Plagemann, Giorgio Grisetti, and Wolfram Burgard. Look-ahead proposals for robust grid-based slam with rao-blackwellized particle filters. *Int. J. Rob. Res.*, 28(2):191–200, 2009.
- [5] T. Palleja, M. Tresanchez, M. Teixido, and J. Palacin. Modeling floor-cleaning coverage performances of some domestic mobile robots in a reduced scenario. *Robot. Auton. Syst.*, 58(1):37–45, 2010.
- [6] Kristopher R. Beevers and Wesley H. Huang. Slam with sparse sensing. In *In IEEE Intl. Conf. on Robotics and Automation*, pages 2285–2290, 2006.
- [7] B. Tribelhorn and Z. Dodds. Evaluating the roomba: A low-cost, ubiquitous platform for robotics research and education. In *Robotics and Automation, 2007 IEEE International Conference on*, pages 1393–1399, Roma.
- [8] Lawrence Erickson, Joseph Knuth, Jason M. O’Kane, and Steven M. LaValle. Probabilistic localization with a blind robot. In *Proc. IEEE International Conference on Robotics and Automation*, 2008.
- [9] Rickard Karlsson, , Rickard Karlsson, and Fredrik Gustafsson. Particle filter for underwater terrain navigation. In *2003 IEEE Workshop on Statistical Signal Processing*, 2003.
- [10] K. Yamazaki, K. Kato, K. Ono, H. Saegusa, K. Tokunaga, Y. Iida, S. Yamamoto, K. Ashiho, K. Fujiwara, and N. Takahashi. Analysis of magnetic disturbance due to buildings. *IEEE Transactions on Magnetics*, 39:3226–3228, 2003.
- [11] Hao Lu, Jiyin Zhao, Xiaomeng Li, and Jianpo Li. A new method of double electric compass for localization. In *Proceedings of the 6th world congress on intelligent control and automation*, 2007.
- [12] Ho-Duck Kim, Sang-Wook Seo, In hun Jang, and Kwee-Bo Sim. SLAM of mobile robot in the indoor environment with digital magnetic compass and ultrasonic sensors. In *Control, Automation and Systems, 2007. ICCAS '07. International Conference on*, pages 87–90, Seoul, 2007.
- [13] S. Suksakulchai, S. Thongchai, D. M. Wilkes, and K. Kawamura. Mobile robot localization using an electronic compass for corridor environment. In *In Proceedings 2000 IEEE International Conference on Systems Man and Cybernetics*, pages 8–11, 2000.
- [14] Janne Haverinen and Anssi Kemppainen. Global indoor self-localization based on the ambient magnetic field. *Robot. Auton. Syst.*, 57(10):1028–1035, 2009.
- [15] Kevin P. Murphy. Bayesian map learning in dynamic environments. In *In Neural Info. Proc. Systems (NIPS)*, pages 1015–1021. MIT Press, 2000.
- [16] Sebastian Thrun, Wolfram Burgard, and Dieter Fox. *Probabilistic Robotics (Intelligent Robotics and Autonomous Agents)*. The MIT Press, 2005.
- [17] Carl Edward Rasmussen and Christopher K. I. Williams. *Gaussian Processes for Machine Learning (Adaptive Computation and Machine Learning)*. The MIT Press, 2005.
- [18] Cyrill Stachniss, Dirk Hähnel, Wolfram Burgard, and Giorgio Grisetti. On actively closing loops in grid-based fastslam. *Advanced Robotics*, 19:2005, 2005.
- [19] Jun S. Liu and Rong Chen. Sequential monte carlo methods for dynamic systems. *Journal of the American Statistical Association*, 93:1032–1044, 1998.
- [20] Jun S. Liu. Metropolized independent sampling with comparisons to rejection sampling and importance sampling. *Statistics and Computing*, 6(2):113–119, 1996.